Journal of Physics and Chemistry of Solids 71 (2010) 199–205

Contents lists available at ScienceDirect

Journal of Physics and Chemistry of Solids

journal homepage: www.elsevier.com/locate/jpcs

Oxidation state characterization in Cr oxides by means of Cr-Kβ emission spectroscopy

G. Tirao [a,b,*], S. Ceppi [a,b], A.L. Cappelletti [c], E.V. Pannunzio Miner [c]

[a] Facultad de Matemáticas, Astronomía y Física, Universidad Nacional de Córdoba, Medina Allende y Haya de la Torre, 5000 Córdoba, Argentina
[b] Consejo Nacional de Investigaciones Científicas y Técnicas (CONICET), Rivadavia 1917, C1033AAJ Ciudad de Buenos Aires, Argentina
[c] INFIQC-CONICET, Departamento de Fisicoquímica, Facultad de Ciencias Químicas, Universidad Nacional de Córdoba, 5000 Córdoba, Argentina

ARTICLE INFO

Article history:
Received 3 June 2009
Received in revised form
27 August 2009
Accepted 12 November 2009

Keywords:
A. Oxides
B. Chemical synthesis
D. Electronic structure

ABSTRACT

High-resolution Kβ spectra of Cr oxide were measured using a non-conventional spectrometer. Theoretical spectra were obtained using the DV-Xα method in order to interpret the Kβ spectrum structures. Kβ spectrum structures were analyzed and spectral parameters show a great sensitivity to the oxidation state and to the Cr–O distance. High-purity samples of CrO_2 were obtained by means of thermal treatment at 513 °C under oxygen pressure of 200 bar. X-ray diffraction patterns show a typical rutile structure, without spurious phases. The CrO_2 data allowed to confirm the linear dependency of the $K\beta_{1,3}$ and $K\beta_{2,5}$ energy positions with the oxidation state. The energy of the $K\beta_{2,5}$ line relative to the $K\beta_{1,3}$ line seems to be a suitable parameter for characterization of the oxidation state. The relative Kβ″ transition probability per Cr–O falls exponentially with Cr–O increasing distance. This behaviour was not found in the literature for Cr oxides.

1. Introduction

Chromium occurs in two common oxidation states in nature, found as ions Cr^{3+} and Cr^{6+}. The Cr^{6+} is toxic to most organisms, carcinogenic in animals, and causes irritation and corrosion of the human skins. It is highly soluble in water and forms the mono- and divalent oxyanions, chromate (CrO_4^{2-}) and dichromate ($Cr_2O_7^{2-}$), respectively, depending on its concentration and pH. Due to the fact that it is only weakly sorbed onto inorganic surfaces, Cr^{6+} is mobile in nature. On the other hand, Cr^{3+} is readily precipitated or sorbed on a variety of inorganic and organic substrates at neutral or alkaline pH. Cr^{6+} is about one hundred times more toxic than Cr^{3+}.

Cr^{4+} ion is less common than the others and has been the focus of interest during the last few years since CrO_2 was found to be a half-metallic ferromagnet [1,2]. It has been used in random access memories for computers, speed sensors, read sensors for magnetic disc drives and magneto-optical recording, among other applications [3,4]. Recently, their magnetorresistance has been well established [5] and has made it one of the most promising candidates in the development of a new generation of spintronic devices [6,7]. However, there are some limitations related to its synthesis and purity degree, obtained using conventional methods, along with its metastable character. This causes difficulties for technological uses. Furthermore, ternary oxides containing Cr^{4+} have interesting properties from an electronic and magnetic point of view [8,9]. Some other compounds with A_2CrO_4 and A_3CrO_5 stoichiometries (where A=Sr, Ba) have been synthesized and they show interesting magnetic properties, although the role of Cr^{4+} has not been yet established with certainty [10].

The chemical effects on X-ray emission spectroscopy (XES) have been known for many years, and they have been often used as a probe of chemical bonding [11]. The use of XES to determine the valence states of first-row transition elements is based on measurements of X-ray energy shifts, satellite lines, variation of line shapes and relative intensities. The energy centroids and line shapes vary not only with oxidation state but also with chemical bonding for the same oxidation state. The electronic transitions from the molecular orbitals (with electronic populations of incomplete shell of Cr and O) to a core-level are suitable candidates for chemically sensitive fluorescence lines, since the character of the molecular orbitals changes markedly between different chemical species, and its influence can be clearly observed in the structure of the emission spectrum. The energy Kβ′ line relative to the $K\beta_{1,3}$ line has been found to shift by <0.1 to ~ 2 eV for V, Cr, Mn, and Fe, depending on the oxidation state, coordination number, and bonding species [12–19]. However, changes are so subtle that oxidation state cannot be simply determined by XES at the resolution obtainable with conventional wavelength-dispersive detectors, with an energy resolution

* Corresponding author at: Facultad de Matemáticas, Astronomía y Física, Universidad Nacional de Córdoba, Medina Allende y Haya de la Torre, 5000 Córdoba, Argentina. Tel.: +54 351 433 4051; fax: +54 351 433 4054.
E-mail address: gtirao@famaf.unc.edu.ar (G. Tirao).

0022-3697/$ - see front matter © 2009 Elsevier Ltd. All rights reserved.
doi:10.1016/j.jpcs.2009.11.004

around 20 eV. These measurements require high-precision intensity scans using high-resolution wavelength spectrometers [20,21] in order to detect the spectral parameters changes due to the chemical environment.

The study of the spectroscopic features of Cr^{4+}, along with research conducted on Cr^{3+} and Cr^{6+}, is very interesting for technological application, since a complete characterization of these ions would allow to characterize the chemical environment of Cr ions, including the oxidation state, ligand type and bond length, in multiple binary and ternary compounds, as well as the study of the stability of Cr^{4+} in different structures. This is possible due to the dependency of the spectrum of Cr-Kβ with its chemical environment.

In this work we describe the synthesis of CrO_2 and the interpretation of the emission spectrum of Cr-Kβ, comparing it with the spectra already established for metallic Cr and the oxides of Cr^{3+} and Cr^{6+}. High-resolution Kβ emission spectra of chromium oxides were measured using a non-conventional spectrometer [21] with a conventional X-ray tube. The experimental data were analyzed in order to characterize the dependence of energy lines and intensities with oxidation state, and also were interpreted in terms of molecular orbital theory with DV-Xα calculations [22]. The measured Kβ emission data for Cr^{4+} was useful to show their behaviour related to the other chromium oxides and to elucidate some discrepancies concerning the spectral parameters among different experimental works.

2. Sample preparation

The Cr, Cr_2O_3, CrO_3 samples used were commercial powders of high purity, 99.9%, 99.5% and 99.998%, respectively, supplied by Strem Chemicals Inc.

2.1. Synthesis of CrO_2

The CrO_2 sample was synthesized as a polycrystalline powder by thermal decomposition of powdered CrO_3 in a capsule of Au foil, under O_2 pressure of 200 bar. Temperature was kept at 513 °C for 10 h; heating and cooling rates were 3 °C min^{-1}. As noted by other authors, CrO_2 has a very narrow stability field. Martinez et al. [23] synthesized $Cr_{1-x}Mn_xO_2$ at 525 °C, the ideal synthesis temperature. In this work, under an O_2 pressure of 200 bar, and at the usual temperatures, ~12 °C above 513 °C, small amounts of Cr_2O_3 were detected. In the same way, CrO_3 and Cr_2O_5 (among other chromium oxides with mixed oxidation states) were formed at 500 °C. The temperature difference respect to that observed by Martinez et al. [23] might be due to the present of Mn in their system, where the thermal stability of doped Cr^{4+} oxide was apparently enhanced.

2.2. Sample structure refinement

The identity and purity of the synthesis product was checked by performing Rietveld analyses of the powder X-ray diffraction (PXRD) pattern taken with a conventional PANalytical XPERT Pro diffractometer, using Cu-Kα radiation obtained at 40 kV and 40 mA. The pattern was measured between 10° and 120° (2θ), with step of 0.02° (2θ) and counting time of 5 s/step. The Rietveld analyses were performed with FullProf [24] using a pseudo-Voigt function for peak-shape modeling. Background was fitted with a six-degree polynomial function and the starting structural model was that proposed by Burdett et al. [25]. Refined values, including unit-cell parameters, atomic displacement parameters, atomic positions and profile parameters, results are listed in Table 1.

3. Kβ emission spectrum

3.1. Theoretical calculations

Theoretical calculations were performed using the Discrete Variational Xα (DV-Xα) MO method [26]. It is assumed that the single electron wave function for a molecular orbital can be considered as a linear combination of atomic orbitals (AO) of isolated atoms. The linear combination coefficients are determined variationally where all the integrations are calculated using the DV method [27]. The DV-Xα method presents some advantages over other theoretical methods for calculations of electronic transition probabilities in molecules [28]. The most important fact is that it allows calculating the multi-center integral easily. As a result, the dipole matrix element included in the X-ray emission probability in the dipolar approximation can be rigorously calculated using MO wave functions numerically obtained from DV-Xα cluster calculations. The validity of this integration method has been tested by calculating the X-ray emission rates [29]. In addition, it is possible to include in the DV-Xα method the relaxation effect using the Slater's "transition state" (TS) concept [30].

To perform the theoretical calculations, it is essential to know the molecular symmetry, the bond length between Cr–O and the angles of O–Cr–O bonds. These data were obtained by Rietveld profile refinement of measured X-ray diffraction patterns of metallic Cr and chromium oxides. Table 1 lists the values of the structural parameters only for the CrO_2 synthesized, with the averages bond distances, since the clusters are not perfectly symmetrical.

In this work theoretical calculations of the Kβ emission spectra were performed including the TS concept, using the octahedral clusters (O_h) CrO_6^{9-} and CrO_6^{8-} for the Cr^{3+} and Cr^{4+}, respectively, and tetrahedral cluster (T_d) CrO_4^{2-} for Cr^{6+}. As explained above, these different clusters present some symmetry distortions which were taken into account in the calculations. On the other hand, in order to simplify the MO nomenclature, designation corresponding to symmetric clusters was used. These results were applied to identify the transition origin in terms of MO theory and to calculate the atomic orbital contributions to the MO as well as relative transition rates and relative energies.

3.2. Experimental measurements

Different oxidation states of Cr in chromium oxides were studied by means of high-resolution Kβ emission spectroscopy. Spectra were obtained with a non-conventional spectrometer, based on quasi-back-diffraction geometry. This spectrometer is similar to one installed at National Synchrotron Light Laboratory—LNLS (Campinas, Brazil) [21], which was previously used to measure high-resolution Kβ spectra of Cr and P compounds [20,31]. It is based on a spherically focusing Si(1 1 1) crystal analyser operated at nearly back-diffraction geometry in order to achieve high energy resolution. The diameter of the Rowland circle corresponds to the curvature radius of the analyser of (415 ± 2) mm. The large effective area of the analyser allows it to collect scattered radiation in a solid angle up to 10 msr. The Bragg angle corresponding to the Cr-$K\beta_{1,3}$ line is 85.86° for the Si(3 3 3) reflection.

The whole spectrometer (sample holder, analyser and detector) is mounted on an adapted Philips horizontal goniometer PW1380 which is driven by a stepping motor with angular step of 9 arcsec. The spectrometer is enclosed in an evacuated chamber, in order to avoid X-ray attenuation and scattering from air. The measurements were performed at conventional 45–45° geometry.

Table 1
Structural parameters, bond distances, angles and agreement indices, refined by Rietveld analyses of PXRD data of CrO_2 sample.

Site/atom	B_{iso}	Atomic coordinates			Cr–O distances [Å]	O–Cr–O angles (°)
2*a* Cr	0.341(7)	0	0	0	4 × 1.879(5)	3 × 89.7(1)
4*f* O	2.61(3)	0.5230(5)	0.1648(8)	0	2 × 1.939(6)	3 × 90.3(1)

S.G.: $P4_2/mnm$,**Cell parameters** [Å]: $a=b=4.4185(3)$, $c=2.9149(2)$.
$R_{wp}=12.9-R_{Bragg}=4.4-\chi^2=2.1$

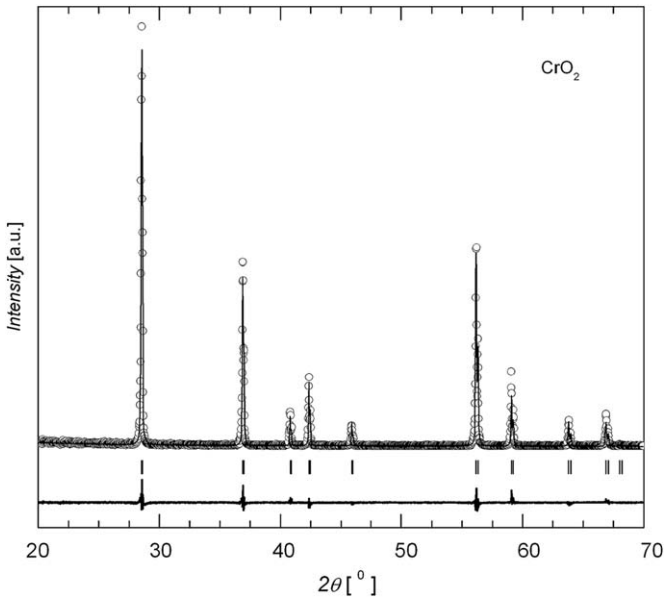

Fig. 1. X-ray powder diffraction pattern of CrO_2. (○): Experimental data. (—): calculated profile by the Rietveld refinement, and their difference at the bottom. The vertical lines correspond to the positions of Bragg reflections.

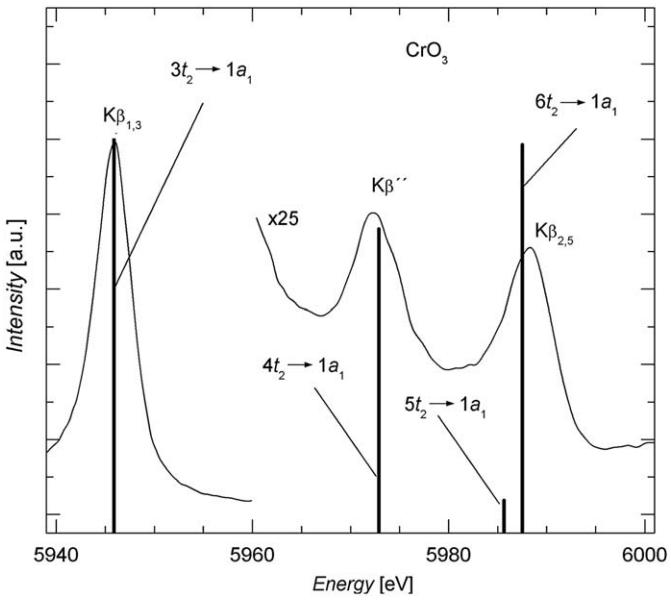

Fig. 2. Cr-Kβ emission spectrum of CrO_3. (—): Experimental data. Vertical lines show theoretical emission lines predicted by the DV-Xα method using the Slater's transition state. These lines have been shifted to match the energy of the main peak. The corresponding MOs involved in the transitions are indicated for each line.

The whole spectrum from a cobalt-target X-ray conventional tube, operated at 35 mA and 40 kV, was used as irradiation source with a fluence of around $\sim 10^{11}$ (photons/seg/mm^2/0.5 keV(BW)/mA).

The high-resolution Kβ emission spectra were recorded by scanning, in steps of about 0.35 eV around the main line, the analyser and the detector synchronously. With a spot size of 7 mm^2, the measured counting rate at the $K\beta_{1,3}$ line was of around 450 counts s^{-1}, and the signal-to-background ratio was better than 35. The resolution of this spectrometer was determined to be 3.3 eV for the Cr-$K\beta_{1,3}$ line (for calculation details see Ref. [21]), and the energy scale was calibrated using the value of the $K\beta_{1,3}$ line of Cr^0 given by Bearden [32] ($EK\beta_{1,3}$=5946.71 eV). To calculate the spectral parameter, the spectra were first normalized to a constant value for the maximum of $K\beta_{1,3}$ line. In the Kβ″ and $K\beta_{2,5}$ region, the background was removed using a lineal function, instead of a more sophisticated fitting curve. Then Voigt functions were fitting in order to reproduce the peaks features. The experimental errors of the studied spectral parameters were determined from the fitting errors.

4. Results and discussion

The synthesized phase of CrO_2 is isostructural with rutile, and no impurities were apparent within the detection limits of the diffraction technique (Fig. 1). The structural parameters obtained, were compared with results of other authors [25,33] and show a good agreement. Values of the refined parameters, as well as bond distances and angles, are listed in Table 1. It can be note that the CrO_6^{8-} is not perfectly octahedral. The distortion of the oxygen coordination octahedral leads to a splitting of the t_{2g} level (Jahn–Teller distortion), but this splitting was not visible in Kβ emission spectra since the 3*d* orbital does not measure directly.

The main Kβ lines originate in the $3p \rightarrow 1s$ transition of the central metallic atom. For Cr-compounds, with 3*d* unpaired electrons, the Kβ emission is split into a doublet composed of the main $K\beta_{1,3}$ line and a less intense, low-energy Kβ′ satellite, whose origin is the 3*p*3*d* exchange coupling. At energies higher than that of $K\beta_{1,3}$ line, two structures of lines Kβ″ and $K\beta_{2,5}$ appear. This spectrum is shown in Fig. 2 for CrO_3 oxide and most of its features can be interpreted by the MO theory, with the exception of the Kβ′ satellite line which is due to the 3*p*3*d* exchange coupling [34,35]. For clusters with T_d (O_h) symmetry, the main $K\beta_{1,3}$ line originates in the $3t_2 \rightarrow 1a_1$ ($3t_{1u} \rightarrow 1a_1$) transition which is equivalent to the $3p \rightarrow 1s$ transition of the central metallic atom. The Kβ″ line corresponds to the $4t_2 \rightarrow 1a_1$ ($4t_{1u} \rightarrow 1a_1$) transition. From the theoretical orbital populations shown in Table 2, it can be observed that in $4t_2$ and the $4t_{1u}$ orbitals are mainly populated by oxygen 2*s* electrons. The $K\beta_{2,5}$ band originates from transitions between the valence band and 1*s* metallic orbital. The valence bands of the chromium compounds are composed of the $1e$, $6a_1$, $5t_2$, $6t_2$ and $1t_1$ molecular orbitals for tetrahedrally coordinated chromium, while for octahedrally coordinated chromium are composed by $6a_{1g}$, $1t_{2g}$, $3e_g$, $5t_{1u}$, $6t_{1u}$, $1t_{1g}$ and $2t_{2g}$ molecular orbitals. Neglecting quadrupolar transitions, the $6t_2 \rightarrow 1a_1$ ($5t_{1u} \rightarrow 1a_1$) transition and the less

Table 2
Atomic orbital contributions to the molecular orbitals of the octahedral clusters (O_h) CrO_6^{8-} for the Cr^{4+}, and tetrahedral cluster (T_d) CrO_4^{2-} for Cr^{6+}.

Compounds	MO	AO orbital population (%)				
		Cr-3*p*	Cr-4*p*	Cr-3*d*	O-2*s*	O-2*p*
CrO_2	$3t_{1u}$	96.4	2.5		0.7	0.4
	$4t_{1u}$	1.7	−0.3		98.0	0.6
	$5t_{1u}$	2.0	−1.1		0.0	99.1
	$6t_{1u}$	0.4	−0.5		0.5	99.6
CrO_3	$3t_2$	97.9	0.1	0.0	1.0	1.0
	$4t_2$	1.1	1.5	3.2	93.7	0.5
	$5t_2$	0.1	−0.2	33.6	2.5	64.0
	$6t_2$	0.5	5.4	0.1	0.5	93.5

intense $5t_2 \rightarrow 1a_1$ ($6t_{1u} \rightarrow 1a_1$) transition are the most important contributions to the $K\beta_{2,5}$ peak for tetrahedral (octahedral) coordination. In these molecular orbitals, the atomic orbital contributions are mainly of oxygen-2*p* and metal-3*d* for T_d symmetry. For O_h symmetry the only contribution is from oxygen-2*p* (see Table 2). These observed features for octahedral symmetry with the experimental spectrum of CrO_3 oxide are shown in Fig. 2. Koster and Mendel [36] proposed that the $K\beta_{2,5}$ peak have contributions of transitions from metal-3*d* to metal-1*s* only when there are 3*d* electrons not used in bond formation. This observation do not agree with the present MO calculations and do not show a dependence on the molecular symmetry (see Table 2), but agree with results of Tsutsumi et al. [34]. These MO contributions to Kβ emission lines also agree with the results of Suzuki et al. [37] and Lenglet et al. [38] who used the DV-Xα and MS-Xα methods [39], respectively, to calculate and interpret the experimental X-ray emission spectra. Therefore, the $K\beta_{2,5}$ features are influence by the coordination symmetry in Cr oxide, as shown in Table 2. An analysis of its intensity is complicated [40], but Eba and Sakurai [41] establish a dependency with the coordination number.

The Kβ″ line is originated from transitions of molecular orbital, with mainly contribution of ligand-2*s*, to the atomic orbital 1*s* of the central atom. Thus, its energy has information about the type of atom that is bound to the emitting atom, whereas its intensity is related to the number of ligand atoms and the distance between them and the emitting atom [42]. This transition could be considered as an *interatomic transition* between the ligand and the principal atom. On the other hand, the $K\beta_{2,5}$ band is formed by transitions filling the metal-1*s* vacancy from molecular orbitals with metal-3*d* and/or metal-4*p* character along with ligand-2*p* or ligand-3*p* character. Then, the $K\beta_{2,5}$ band involves a valence-to-core transitions which are chemically sensitive and can be used to determine the oxidation state [40]. Satellite lines of the Cr-Kβ emission spectra for Cr^0 and the studied oxides are shown in Fig. 3.

The $K\beta_{1,3}$ peak position shift to lower energy with increasing oxidation state was observed by several authors [20,36,38,42,43]. According to Tyson et al. [44], an increase in the oxidation state should lead to a lowering of the 3*p*–1*s* transition energy; because the 3*d* electron charge localized around the metal decreases and the core electrons become weaker screened. Thus, both the initial 3*p* and final 1*s* states shift to higher binding energies, being larger the 3*p* shift. If the bond character and coordination remain approximately the same, the $K\beta_{1,3}$ shift could be expected to behave linearly, as pointed by Koster and Mendel [36]. In a recent work, Glatzel and Bergmann [13] show that the shift of the $K\beta_{1,3}$ line is not caused by a change in nuclear screening between different oxidation states. The short-range of the (3*p*, 3*d*) exchange interaction makes the $K\beta_{1,3}$ peak position dependent on the exchange interaction between the 3*p* hole and the unpaired spin in the valence shell the K fluorescence line only sensitive to the electron density localized on the metal ion, *i.e.*, the effective number of unpaired 3*d* electrons, related with the oxidation state. A linear dependency between the $K\beta_{1,3}$ peak position and oxidation state is clearly observed in Fig. 4a for the experimental data obtained in this work and by other authors [20,36,38,42,43]. The $K\beta_{1,3}$ line shifts to lower energy by ~ -0.65 eV per increment of unit oxidation state, in agreement with results of these authors. It is worth noting that the value of Torres Deluigi et al. [20] for Cr^{6+} was measured for the K_2CrO_4 compound. This compound was also measured in this work in order to compare with the CrO_3 oxide, giving an indistinguishable value for this spectral parameter. Torres Deluigi et al. [20] pointed some discrepancies with the result of Gamblin and Urch [42], when trying to include the Cr^0 in the linear behaviour as a function of oxidation state, comparing an ionic and metallic solid. However, all the values from different authors [20,36,38,42,43] showed, with a noticeable dispersion, the correct tendency.

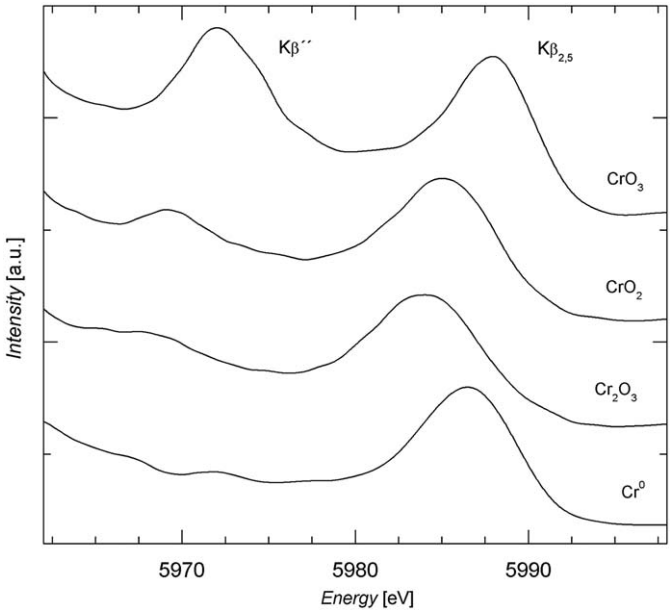

Fig. 3. Satellite lines of the Cr-Kβ emission spectra for Cr^0 and the studied oxides. The measurement was obtained with a high-resolution spectrometer [21], using an X-ray conventional tube. The Kβ″ and $K\beta_{2,5}$ lines are indicated.

The measured values of the $K\beta_{2,5}$ energy position are shown in Fig. 4b with those reported by other authors. A shift to higher energy with increasing oxidation state, ~1 eV per increment of unit oxidation state can be observed. A good agreement with the values of Koster and Mendel [36] and a reasonable dispersion from Ihara's data [43] could be observed in Fig. 4b. A direct comparison with data of Torres Deluigi et al. [20] should be made carefully since the value corresponding to Cr^{6+} was measured in K_2CrO_4 compound, and it could be shifted up to 2 eV depending on the chemical environment with the same oxidation state [20]. In this work, the $K\beta_{2,5}$ energy positions for CrO_3 and K_2CrO_4 differ only in 0.54 eV. Despite the spreading, the satellite line energy shows a similar behaviour to that of Mn-compounds [36,40].

Few authors present experimental data concerning to the features of the Kβ emission spectrum of Cr in CrO_2. Lenglet et al. [38] measured the Cr-Kβ emission spectrum in chromium oxide (Cr^{3+}, Cr^{4+} and Cr^{6+}) with a sequential spectrometer using a molybdenum anode X-ray tube, and in order to obtain good resolution, first-order diffraction from a topaz crystal was used. However, the authors present few result referring to spectral parameters (energy position and intensity) of the main and

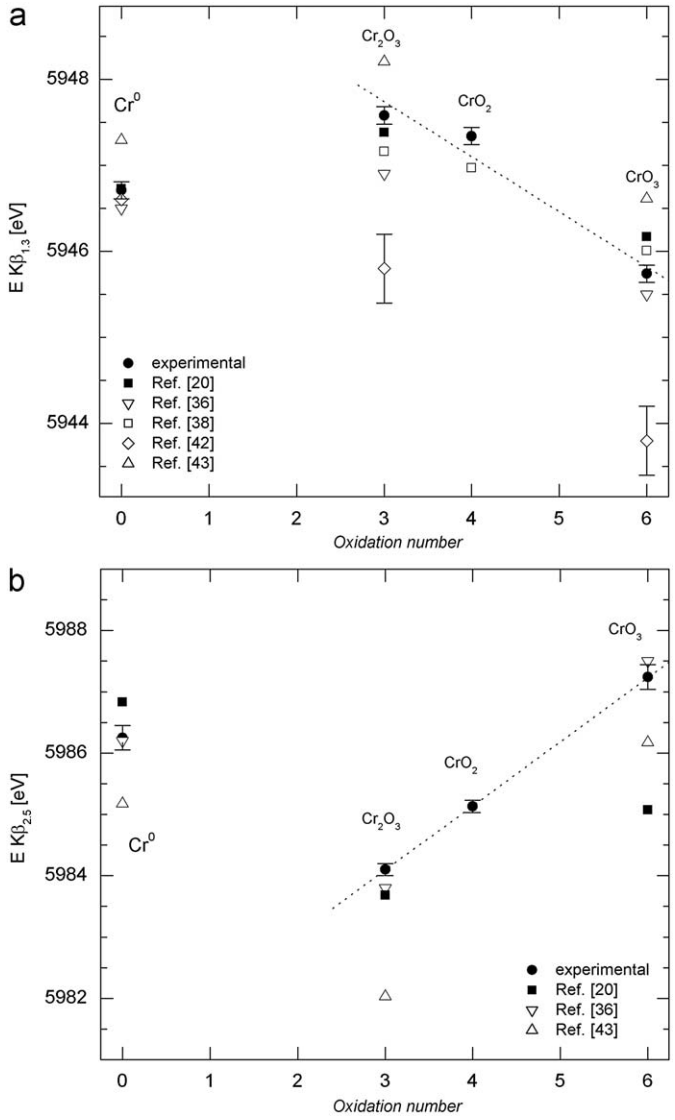

Fig. 4. Energy shift for the $K\beta_{1,3}$ main line (a) and the $K\beta_{2,5}$ satellite line (b) as a function of the oxidation number. The present data are compared with result of other authors. The dashed line is a linear fit to present data. The data of Torres Deluigi et al. [20] for Cr^{6+} correspond to K_2CrO_4.

satellites lines. For the CrO_2 oxide, only the energy positions, relative to Cr^0, of $K\beta_{1,3}$ and $K\beta_{2,5}$ lines were shown. The data obtained in this work for Cr^{4+} confirm the linear dependency of the $K\beta_{1,3}$ and $K\beta_{2,5}$ energy positions with the oxidation states, this trend could not be confirmed with results reported in a previous work [20]. In case of Mn-compounds, which can have more oxidation states, this linear dependency was already observed by some authors [36,40].

The $K\beta_{2,5}$ line shifts due to the change of oxidation state is higher than for the main line $K\beta_{1,3}$, and its intensity is much lower (20–30 times), having some structure also depending on the coordination number [41]. Both lines can be used for valence and coordination characterization. Nevertheless, a more sensitive parameter to the oxidation state characterization is the $K\beta_{2,5}$ energy line relative to the energy $K\beta_{1,3}$ line ($\Delta E\text{-}K\beta_{2,5}$), showing a shift of $\sim$1.7 eV per increment of unit oxidation number, compared to a shift of $\sim$1 eV for the energy $K\beta_{2,5}$ line, a 70% greater than for the $K\beta_{2,5}$ line shift. This feature can be observed in Fig. 5 with a good agreement among different data and a linear dependency with little dispersion is clearly visible. According to

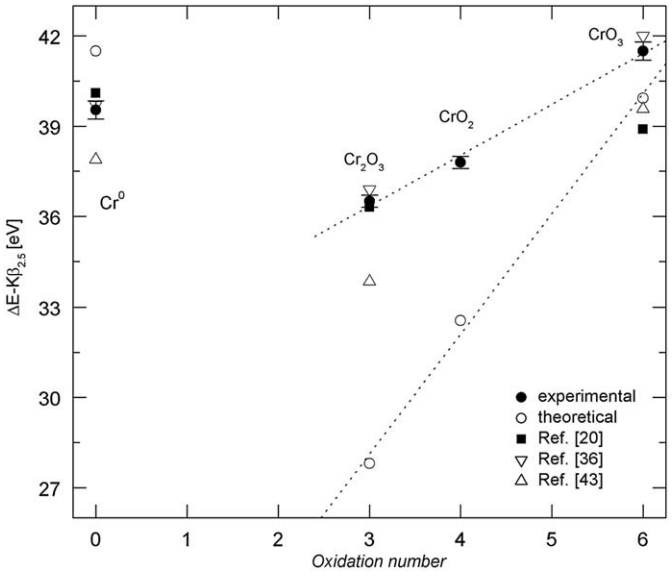

Fig. 5. Energy of the Cr-$K\beta_{2,5}$ line relative to the main line $K\beta_{1,3}$, as a function of the oxidation number for experimental data. Theoretical calculations are also shown. The dashed line represents a linear fit. Values for Cr^{6+} obtained by Torres Deluigui et al. [20] correspond to K_2CrO_4.

Bearden [32], the energy difference between the $K\beta_{2,5}$ and $K\beta_{1,3}$ lines is 39.8 eV for Cr^0, which is very close to the value measured in the present work: (39.5 ± 0.3) eV. Another advantage of using the $\Delta E\text{-}K\beta_{2,5}$ parameter is the lack of sensibilities to the energy calibration without requiring an accurate reference. That is the reason because in Fig. 5 are also presented the theoretical data, showing the same increasing tendency, although with different slope. It is well established the limitation of the DV-Xα method to precisely calculation of emissions lines energies [45]. Theoretical lines have been shifted 33 eV in order to match the energy of the main peak, as shown in Fig. 1, but the errors of the calculated relative energy are considerably smaller (see Fig. 5) and may become within of $\sim$3 eV [28,31].

Assuming that the integrated intensity per Cr of the main Kβ region is chemically invariant [40], the relative Kβ'' transition probability per Cr–O can be calculated normalizing the intensities of the Kβ'' line by the integrated intensity of the main Kβ region (5935–5963 eV) and by the number of oxygen ligands per Cr. This transition probability falls exponentially as a function of the Cr–O bonding length. The same behaviour was found in Mn-compounds [40]. From theoretical calculation, the Kβ'' intensity derives primarily from the metal-*p* character of the initial state wave function [46]. Mukoyama et al. [47] have used Xα calculations to quantitatively estimate crossover intensities, suggesting that most of the strength of the transitions comes from the metal character of the orbitals. In perturbation theory the orbital population of metal-*p* and O-2*s* mixing will depend on the overlap between these wave functions, which have exponential tails. Therefore, the observed correlation between Kβ'' intensity and bond length should vary exponentially with distance [40]. Furthermore, there is a strong dependence of Kβ'' intensity with metal–ligand distance. Theoretical results and the experimental data are shown in Fig. 6, where the exponential decay with Cr–O distance can be clearly observed, with a very good agreement. From Fig. 6 it appears that the relative Kβ'' transition probability could be used to evaluate Cr–O distances to within $\sim$0.1 Å for no sophisticated complexes, considering the error bars and values dispersion, as viewed in the graph. This statement was also found by Bergmann et al. [40] for Mn-compounds. From the value of K_2CrO_4 compound, it can also be

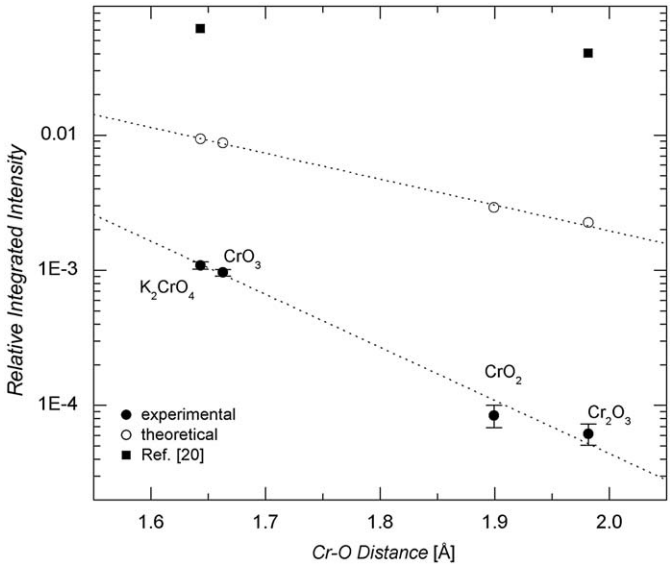

Fig. 6. Measured (●) and calculated (○) relative Kβ″ transition probability as a function of Cr–O distance, for metallic Cr and chromium compounds. Values obtained by Torres Deluigui et al. [20] are also shown. To represent this transition probability, Kβ″ intensities were normalized by the integrated intensity of the main Kβ region and further by the number of O-ligands per Cr. The dashed lines are least-squares fits using exponential type distance dependence.

noticed the great sensitivity to the presence of cation to modify the Cr–O bonding length. On the contrary, for each of the spectral parameters obtained, shown in Figs. 4 and 5, data for K_2CrO_4 and CrO_3 are within the corresponding experimental errors, making them indistinguishable.

5. Conclusion

High-purity and polycrystalline samples of CrO_2 were obtained by thermal treatment of CrO_3 powder, packing in a gold capsule, at 513 °C in 200 bar of oxygen pressure. The X-ray diffraction pattern showed a typical rutile structure, were corner-sharing CrO_6 octahedral clusters are not symmetrical.

High-resolution Kβ spectra of Cr oxides with a Cr in different oxidation states were measured using a non-conventional spectrometer with an X-ray conventional tube as a radiation source. Spectral parameters from these spectra, such as relative energy and normalized intensity, show a great sensitivity to the oxidation state of Cr and to the Cr–O distance. Theoretical parameters were calculated using the DV-Xα method. The calculated spectra obtained using all the cluster information, *i.e.*, the Cr–O bond length and the angles between O–Cr–O bonds, are consistent with the experimental ones. The results provided by the DV-Xα calculation method allow the identification of the MO involved in the electronic transitions and the analysis of origin of changes related to the chemical environment.

Energy positions of the $K\beta_{1,3}$ and $K\beta_{2,5}$ lines show the expected tendency, in agreement with the results of other authors and with present theoretical calculations for $\Delta E\text{-}K\beta_{2,5}$, the relative energy $K\beta_{2,5}$ to the main line $K\beta_{1,3}$. The $K\beta_{1,3}$ shifts towards lower energy with an increase the oxidation states, and the $K\beta_{2,5}$ shifts are in the opposite way. Therefore, the $\Delta E\text{-}K\beta_{2,5}$ as a function of oxidation number seems to be a suitable parameter for characterization of the Cr oxidation state of compounds.

The relative Kβ″ transition probability per Cr–O, theoretical and experimentally calculated, falls exponentially as a function of the Cr–O bonding length. This behaviour has been found for Mn [40], but it has not been yet reported for Cr oxides and compounds. This spectral parameter could be used to evaluate Cr–O distances to within ~0.1 Å, with great sensitivity for the presence of a cation.

The Cr^{4+} experimental data are useful to dispose of the discrepancies concerning the spectral parameter between different experimental works, related to linear tendency and values of $K\beta_{1,3}$ and $K\beta_{2,5}$ lines shift [20,36,38,42,43] and the relative intensity of the $K\beta_{2,5}$ [20,36,43] that exist between different experimental works. There are few experimental data for CrO_2 referred to the features of Kβ emission spectra. In this work, all the relevant spectral parameters were obtained from high-resolution Kβ emission spectra and it was possible to confirm the linear dependency of the $K\beta_{1,3}$ and $K\beta_{2,5}$ energy positions with the oxidation state.

Acknowledgements

Financial supports from the Consejo Nacional de Investigaciones Científicas y Técnicas (CONICET), from the Agencia Nacional de Promoción Científica y Tecnológica (ANPCYT) and from the Secretaría de Ciencia y Técnica de la Universidad Nacional de Córdoba (UNC) are gratefully acknowledged.

References

[1] B.L. Chamberland, The chemical and physical properties of CrO_2 and tetravalent chromium oxide derivatives, Crit. Rev. Solid State Mater. Sci. 7 (1977) 1–31.
[2] K.H. Schwarz, CrO_2 predicted as a half-metallic ferromagnet, J. Phys. F: Met. Phys. 16 (1986) L211–L215.
[3] K. Suzuki, M.P. Tedrow, Longitudinal magnetoresistance of CrO_2 thin films, Appl. Phys. Lett. 74 (1999) 428–429.
[4] P.G. Ivanov, S.M. Watts, D.M. Lind, Epitaxial growth of CrO_2 thin films by chemical-vapor deposition from a Cr_8O_{21} precursor, J. Appl. Phys. 89 (2001) 1035–1040.
[5] J. Dai, J. Tang, Junction-like magnetoresistance of intergranular tunneling in field-aligned chromium dioxide powders, Phys. Rev. B: Condens. Matter Mater. Phys. 63 (2001) 1–9 054434.
[6] S.A. Chambers, Y.K. Yoo, New materials for spintronics, Mater. Res. Soc. Bull. 28 (2003) 706–710.
[7] G.P. Singh, B. Biswas, S. Ram, K. Biswas, Structure and magnetic properties in Ag-stabilized ferromagnetic sensor of CrO_2 nanoparticles, Mater. Sci. Eng., A 498 (2008) 125–128.
[8] D. Groult, C. Martin, A. Maignan, D. Pelloquin, B. Raveau, The "1201" bismuth based cobaltite $Bi_{0.5}Cd_{0.3}Sr_2Co_{1.2}O_{5-\delta}$: a new magnetoresistant spin glass like insulator, Solid State Commun. 105 (1998) 583–588.
[9] E. Castillo-Martinez, A. Durán, M.Á. Alario-Franco, Structure, microstructure and magnetic properties of $Sr_{1-x}Ca_xCrO_3$ ($0 \le x \le 1$), J. Solid State Chem. 181 (2008) 895–904.
[10] T. Baikie, Z. Ahmad, M. Srinivasan, A. Maignan, S.S. Pramana, T.J. White, The crystallographic and magnetic characteristics of Sr_2CrO_4 (K_2NiF_4-type) and $Sr_{10}(CrO_4)_6F_2$ (apatite-type), J. Solid State Chem. 180 (2007) 1538–1546.
[11] A. Meisel, G. Leonhardt, R. Szargan., in: X-Ray Spectra and Chemical Binding, Springer-Verlag, New York, 1989.
[12] Y. Tamaki, Chemical effect on intensity ratios of K-series x-rays in vanadium, chromium and manganese compounds, X-Ray Spectrom. 24 (1995) 235–240.
[13] P. Glatzel, U. Bergmann, High resolution 1s core hole X-ray spectroscopy in 3d transition metal complexes—electronic and structural information, Coord. Chem. Rev. 249 (2005) 65–95.
[14] G. Leonhardt, A. Meisel, Determination of effective atomic charges from the chemical shifts of X-ray emission lines, J. Chem. Phys. 52 (1970) 6189–6197.
[15] D.S. Urch, P.R. Wood, The determination of the valency of manganese in minerals by X-ray fluorescence spectroscopy, X-Ray Spectrom. 7 (1978) 9–11.
[16] D.S. Urch, S. Webber, Fe-$K\beta_{1,3}$ X-ray emission spectra from complexes which contain ferric iron in unconventional spin states, X-Ray Spectrom. 6 (1977) 64–65.
[17] E. Asada, T. Takiguchi, Y. Suzuki, The effect of oxidation state on the intensities of $K\beta_5$ and Kβ′ of 3d-transition elements, X-Ray Spectrom. 4 (1975) 186–189.
[18] Y. Goshi, A. Ohtsuka, The application of chemical effects in high resolution X-ray spectrometry, Spectrochim. Acta, Part B 28 (1973) 179–188.
[19] N. Kallithrakas-Kontos, X-ray chemical shift determination by energy dispersive detection, Spectrochim. Acta, Part B 51 (1996) 1655–1659.
[20] M. Torres Deluigi, G. Tirao, G. Stutz, C. Cusatis, J.A. Riveros, Dependence with the oxidation state of X-ray transition energies, intensities and natural line widths of CrKβ spectra, Chem. Phys. 325 (2006) 477–484.

[21] G. Tirao, G. Stutz, C. Cusatis, An inelastic X-ray scattering spectrometer at LNLS, J. Synchrotron Rad. 11 (2004) 335–342.
[22] H. Adachi, M. Tsukada, C. Satoko, Discrete variational Xα cluster calculations. I. Application to metal clusters, J. Phys. Soc. Jpn. 45 (1978) 875–883.
[23] B. Martínez, J. Fontcuberta, M.J. Martínez-Lope, J.A. Alonso, Magnetoresistance in electron doped $Cr_{1-x}Mn_xO_2$ double exchange ferromagnet, J. Appl. Phys. 87 (2000) 6019–6021.
[24] J. Rodriguez-Carbajal, Recent advances in magnetic structure determination by neutron powder diffraction, Physica B (Amsterdam, Netherlands) 192 (1993) 55–69.
[25] J.K. Burdett, G.J. Miller, J.W. Richardson, J.V. Smith, Low-temperature neutron powder diffraction study of chromium dioxide and the validity of the Jahn–Teller viewpoint, J. Am. Chem. Soc. 110 (1988) 8064–8071.
[26] H. Adachi, S. Shiokawa, M. Tsukada, C. Satoko, S. Sugano, Discrete variational Xα cluster calculations. III. Application to transition metal complexes, J. Phys. Soc. Jpn. 47 (1979) 1528–1537.
[27] F.W. Averill, D.E. Ellis, An efficient numerical multicenter basis set for molecular orbital calculations: application to $FeCl_4$, J. Chem. Phys. 59 (1973) 6412–6418.
[28] T. Mukoyama, Hartree–Fock–Slater method for materials science, in: H. Adachi, T. Mukoyama, J. Kawai (Eds.), The DV-Xα Method for Design and Characterization of Materials, Springer-Verlag, Berlin, 2006, p. 163.
[29] T. Mukoyama, K. Taniguchi, H. Adachi, The discrete variational calculations of the overlap integrals and the dipole matrix elements, Bull. Inst. Chem. Res. Kyoto Univ. 62 (1984) 13–16.
[30] J.C. Slater, Quantum Theory of Molecules and Solids, vol. 4, McGraw-Hill, USA, 1974.
[31] S. Ceppi, G. Tirao, G. Stutz, J.A. Riveros, Chemical environment effects on the Kβ emission spectra in P compounds, Chem. Phys. 354 (2008) 80–85.
[32] J.A. Bearden, X-ray wavelengths, Rev. Mod. Phys. 39 (1967) 78–124.
[33] B.R. Maddox, C.S. Yoo, D. Kasinathan, W.E. Pickett, R.T. Scalettar, High-pressure structure of half-metallic CrO_2, Phys. Rev. B: Condens. Matter Mater. Phys. 73 (2006) 144111 1-9.
[34] K. Tsutsumi, H. Nakamori, K. Ichikawa, X-ray Mn Kβ emission spectra of manganese oxides and manganates, Phys. Rev. B: Condens. Matter Mater. Phys. 13 (1976) 929–933.
[35] G. Peng, F.M.F. deGroot, K. Hämäläinen, J.A. Moore, X. Wang, M.M. Grush, J.B. Hastings, D.P. Siddons, W.H. Armstrong, O.C. Mullins, S.P. Cramer, High-resolution manganese X-ray fluorescence spectroscopy oxidation-state and spin-state sensitivity, J. Am. Chem. Soc. 116 (1994) 2914–2920.
[36] A.S. Koster, H. Mendel, X-ray Kβ emission spectra and energy levels of compounds of 3d-transition metals–I, J. Phys. Chem. Solids 31 (1970) 2511–2522.
[37] C. Suzuki, J. Kawai, H. Adachi, T. Mukoyama, Electronic structures of 3d transition metal (Ti–Cu) oxides probed by a core hole, Chem. Phys. 247 (1999) 453–470.
[38] M. Lenglet, M. Sakout, J. Dürr, G. Wrobel, X-ray CrKβ emission and K absorption spectra in mixed copper chromium oxides, Spectrochim Acta, Part A 46 (1990) 1101–1106.
[39] J.C. Slater, Statistical exchange-correlation in the self-consistent field, Adv. Quantum Chem. 6 (1972) 1–92.
[40] U. Bergmann, C.R. Horne, T.J. Collins, J.M. Workman, S.P. Cramer, Chemical dependence of interatomic X-ray transition energies and intensities–a study of Mn Kβ″ and $Kβ_{2,5}$ spectra, Chem. Phys. Lett. 302 (1999) 119–124.
[41] H. Eba, K. Sakurai, Site occupancy determination for manganese in some spinel-type oxides by Kβ X-ray fluorescence spectra, J. Solid State Chem. 178 (2005) 370–375.
[42] S.D. Gamblin, D.S. Urch, Metal Kβ X-ray emission spectra of first row transition metal compounds, J. Electron. Spectrosc. Relat. Phenom. 113 (2001) 179–192.
[43] J. Iihara, T. Omori, K. Yoshihara, K. Ishii, Chemical effects in chromium L X-rays, Nucl. Instrum. Methods: Phys. Res., Sect. B 75 (1993) 32–34.
[44] T.A. Tyson, Q. Qian, C.-C. Kao, J.-P. Rueff, F.M.F. de Groot, M. Croft, S.-W. Cheong, M. Greenblatt, M.A. Subramanian, Valence state of Mn in Ca-doped $LaMnO_3$ studied by high-resolution Mn Kβ emission spectroscopy, Phys. Rev. B: Condens. Matter Mater. Phys. 60 (1999) 4665–4673.
[45] H. Adachi, K. Taniguchi, Discrete variational Xα cluster calculations. IV. Application to X-ray emission study, J. Phys. Soc. Jpn. 49 (1980) 1944–1953.
[46] J.B. Jones, D.S. Urch, Metal–ligand bonding in some vanadium compounds: a study based on X-ray emission data, J. Chem. Soc., Dalton Trans. (1975) 1885–1889.
[47] T. Mukoyama, K. Taniguchi, H. Adachi, Interatomic contributions to molecular x-ray emission rates, Phys. Rev. B: Condens. Matter Mater. Phys. 41 (1990) 8118–8121.